High-Performance Chip-Assisted Microwave Photonic Functionalities

Yang Liu, David Marpaung, Benjamin J. Eggleton, *Fellow, IEEE*, and Amol Choudhary

***Abstract*— Integrated microwave photonics (IMWP) is poised to release the bottlenecks in modern wireless communication systems. The manipulation of microwave signals in the optical domain offers key advantages of broad bandwidth, reconfiguration, and fast tuning speeds. However, in current IMWP devices, there are some challenges that need to be overcome. These include the ∼1 GHz frequency resolution of the IMWP functionalities, limited by the on-chip photonic functional devices' performance, which has prompted research into on-chip stimulated Brillouin scattering (SBS) to achieve sub-30 MHz signal processing capabilities. Equally important, the performance metrics including the noise figure, dynamic range, and the insertion loss, need to be improved before commercial deployment. While SBS offers significant advantages of high resolution and reconfigurability, there is potential for improved signal-to-noise ratios and, therefore, to obtain a low noise figure. In this letter, we present an overview of recent approaches for achieving high-performance IMWP functionalities, including SBS-induced noise management and the optimized MWP link configurations.**

***Index Terms*— Microwave photonics, integrated optics, wireless communications, stimulated Brillouin scattering, noise figure, silicon nitride ring resonator.**

I. Introduction

MODERN communication networks are putting stringent demands on the bandwidth, tuning speeds and reconfigurability of basic microwave components such as filters, phase shifters and delay lines. These increasingly demanding performance requirements have motivated considerable investment in the development of photonic-based microwave signal processing functionalities [1], [2] that can address these needs in applications. To complement other RF components, a recent focus has been on integrating functionalities [3] on a chip-scale device, resulting in several demonstrations based on linear optics, such as microring resonators [4] and nonlinear optics, using stimulated Brillouin scattering (SBS) [5]. While impressive progress in compactness and functionalities have been achieved, limited efforts have been made to optimize the underlying analog photonic link in addition to the functionalities. Also, the spontaneous noise added by active processes such as the SBS gain process in the passbands can be detrimental to the signal fidelity, especially in the case where the filter is operated in a regime of high gain and low RF signal power [6], which has motivated additional efforts to minimize the noise within the SBS processing bandwidth.

In this letter, we review recent progress in the optimization of the critical metrics such as noise figure, dynamic range and link loss of integrated microwave photonic functionalities

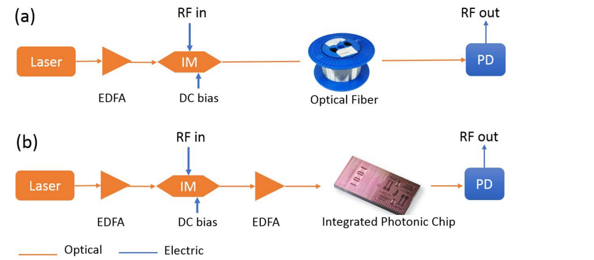

Fig. 1. (a) A typical analog photonic link, and (b) an optimized link with a photonic chip (for example ring resonators), to realize a functionality. IM: Intensity modulator, EDFA-Erbium Doped Fiber amplifier, PD-Photodetector.

II. Metrics of an IMWP Analog Photonic Link

A typical analog photonic link consists of a laser, an electro-optic modulator and the photodetector as shown in Fig. 1(a). The quality of the RF signal can be impaired due to the insertion loss, the added noise and the device response nonlinearities present in the system thus limiting the link gain (G), the noise figure (NF), and the spurious free dynamic range (SFDR) of the link [7], respectively. The NF defined as the degradation of the signal to noise ratio (SNR) in the signal chain, can be calculated as:

$$\mathrm{NF} = \mathrm{P_N} - \mathrm{G} + 174 \quad (1)$$

where, P_N is the measured noise power spectral density (PSD) in dBm/Hz and G is the link gain (dB). The three main sources of noise in an analog photonic link are the relative intensity noise (P_{RIN}) related to the amplitude fluctuations of the laser, the shot noise (P_{shot}) related to random arrivals of the photons in the photodetector and the thermal noise (P_{th}) due to the random thermal motion of charge carriers.

The SFDR represents the degree of the signal distortions and nonlinearity caused by the link nonlinearity at the strongest spurious frequencies. It is typically measured using a two-tone test [3]. The powers of the 2^{nd}-order, 3^{rd}-order spurs and the fundamental frequency are plotted as a function of the input power. The intercept points of the extrapolated curves for the

Manuscript received June 20, 2018; revised July 18, 2018; accepted July 23, 2018. Date of publication July 3, 2018; date of current version November 6, 2018. This work was supported in part by ARC under Grants DE170100585, FL120100029, and CE110001018 and in part by AFOSR/AOARD under Grant FA2386-16-1-4036. *(Corresponding author: Amol Choudhary.)*

Invited paper for the Integrated Microwave Photonics Special Issue.

Y. Liu, B. J. Eggleton, and A. Choudhary are with the School of Physics, Institute of Photonics and Optical Science, The University of Sydney, Sydney, NSW 2006, Australia, and also with The University of Sydney Nano Institute, The University of Sydney, Sydney, NSW 2006, Australia (e-mail: yliu3472@uni.sydney.edu.au; benjamin.eggleton@sydney.edu.au; amol.choudhary@sydney.edu.au).

D. Marpaung is with the Faculty of Science and Technology, University of Twente, 7522 NB Enschede, The Netherlands (e-mail: d.a.i.marpaung@utwente.nl).

Color versions of one or more of the figures in this letter are available online at http://ieeexplore.ieee.org.

Digital Object Identifier 10.1109/LPT.2018.2859951

1041-1135 © 2018 IEEE. Translations and content mining are permitted for academic research only. Personal use is also permitted, but republication/redistribution requires IEEE permission. See http://www.ieee.org/publications_standards/publications/rights/index.html for more information.

2^{nd} and 3^{rd}-order spurs with the fundamental give the input intercept point IIP_2 and IIP_3, respectively, which allows for the calculation of the second- and third-order SFDR in dB, given by:

$$SFDR_2 = 1/2(IIP_2 - NF + 174) \quad (2)$$

$$SFDR_3 = 2/3(IIP_3 - NF + 174) \quad (3)$$

The introduction of a photonic chip into the link, enables the 'functionalization' of the link as shown in Fig.1 (b), however this adds extra insertion loss, thus reducing the link gain. This also has the effect of increasing the noise figure as seen from equation (1) and reducing the $SFDR_2$ and $SFDR_3$ as seen from equation (2) and (3). Furthermore, in the case of on-chip SBS, the spontaneous noise power would also result in worsening the NF and SFDR. Therefore, strategies are required to a) limit the effect of SBS noise on the link performance, and b) optimize the combination of the optimized link configurations and the functionality and are discussed below.

III. Minimizing Noise in SBS-Based RF Photonics

SBS is a nonlinear optical interaction between a counter-propagating pump and signal wave and the generated acoustic wave, which results in narrowband amplification and loss at the Stokes (lower) and the anti-Stokes (higher) frequency, respectively [5]. On-chip SBS has been reported in several platforms [8]–[10] with gains more than 50 dB [11] being achieved. However, such high gains in turn result in an increased level of spontaneous noise that can degrade the signal-to-noise ratio. Techniques that minimize this noise for applications in RF photonics are:

A. RF Interference

One possible avenue for minimizing SBS noise in RF applications is to use low SBS gain which introduces less noise. This is typically achieved by using the emerging concept of RF interference, where two RF signals interfere at photodetection [12]. This relies on the encoding of the RF signal onto the optical domain that results in two sidebands with controllable amplitudes and phase relations. In the case a phase modulator is used, two equal sidebands with a broadband π-offset are formed that interfere destructively at photodetection. However, when a small SBS gain is applied to one sideband, the symmetry between the sidebands is broken in a very narrow band (i.e. SBS processing bandwidth), resulting in a bandpass filter response [13]. This filter has lower noise and an improvement in selectivity of >10 dB, compared to an MWP bandpass filter based on the SBS gain response only. Using this technique, bandpass filters with a bandwidth reconfigurability of up to 440 MHz and a frequency tunability of up to 30 GHz have been achieved [13] using a chalcogenide chip. Furthermore, using the concept of RF interference, phase-shifters and delay lines using low SBS gains have been developed that will also reduce the added SBS noise within the operating bandwidth [14].

RF interference can also be used to develop high-extinction notch filters using a modulation format which results in two sidebands out-of-phase by π but with unequal amplitudes. Low SBS gain (using chalcogenide waveguides) of ∼1 dB is applied to one of the sidebands which is then attenuated by ∼1 dB thus ensuring that the condition for destructive interference is met within the SBS bandwidth. This results in a notch filter with a rejection ratio >50 dB [15]. The bandwidth of this filter was also tunable from 32-88 MHz and the central frequency was tunable up to 30 GHz. To increase the shape factor of these filters, advanced dispersion compensation techniques were also used to make the bandwidth reconfigurable up to 300 MHz [16]. In these bandstop filters, since the SBS effect is utilized in the stopband, additional SBS noise doesn't affect the RF signal of interest.

B. Anti-Stokes Interactions

Another alternative technique based on the anti-Stokes interactions that can alleviate the side-effects of SBS noise on a signal was proposed by Feng *et al.* [17]. This technique relies on the creation of an optical bandpass filter, using two tailored SBS loss responses (single mode fibers as the gain medium) on either side of the passband. Using this technique, optical filters with selectivity of 20 dB, bandwidth reconfigurable from 0.5-9.5 GHz were achieved, with the added SBS noise being in the stopband thus not impairing the RF signal. This technique can be applied to an analog photonic link to realize high-performance RF photonic bandpass filters.

Recently, a technique [18] has been demonstrated where SBS loss using optical fibers instead of SBS gain as in [13] was used to break the symmetry between two out-of-phase sidebands. The advantage of using SBS loss over SBS gain is that it does not saturate at high input optical signal powers, thus having a higher dynamic range. Also, less spontaneous noise is generated in SBS loss as in this process the thermal phonons' energy is scattered to a higher optical frequency. In [18], bandpass filters with a selectivity of ∼25 dB and an insertion loss of 15 dB were synthesized using SBS loss and SBS gain. An SNR improvement of 8 dB and a dynamic range improvement of 3 dB was observed using SBS loss. This technique is compatible with on-chip SBS [13] and is thus promising for the realization of high-performance microwave photonic functionalities.

C. Separate Pump and Signal Paths

Since a lot of the SBS noise is introduced by the spontaneously generated photons when applying a strong optical pump, Kittlaus *et al.* [19] have recently reported an RF filter that relies on the separation of the pump and the signal paths using a silicon photonic-phononic emitter receiver waveguide geometry. In this scheme, the RF information is encoded using an intensity modulator into the optical domain which is sent through the emitter waveguide, where the acoustic waves for signal processing are generated. This information gets transferred to the acoustic phonons that propagate to the receiver waveguide and phase modulate the probe light in the receiver waveguide, imparting a transfer function determined by the acoustic waves. The output optical signal is then down-converted to the RF domain and is measured as a bandpass filter response. Filters with a linewidth of 5 MHz and selectivity of ∼30 dB were achieved. The noise figure, $SFDR_3$ and the link gain of the filter were measured to be 50 dB, 99.3 dB/$Hz^{2/3}$ and −2.3 dB, respectively. This technique has the advantage of separating the spontaneous noise source from the signal path, which suggests an efficient way to mitigating the effects of SBS noise that gets transferred to the RF domain.

IV. Optimization of the System Metrics

To increase the link gain of the analog photonic link, it is possible to use a high-power laser or several optical amplifier stages to compensate for the losses due to electro-optic conversion and the insertion losses of various components. However, this has the effect of increasing the NF due to an increased P_{RIN}, P_{shot} and added amplifier spontaneous noise. Low-biasing of the intensity modulator is a commonly-used technique to overcome the degradation in the noise performance [7]. This relies on operating the modulator close to the null point, where the noise power falls off at a faster rate than the link gain. This can be explained by the faster reduction rate of the dominant RIN noise, compared to the rate of decrease of the link gain, when the optical carrier transmission is tuned towards the null point. With this optimization technique, links with G=0 dB, NF $<$ 10 dB and $SFDR_3 = 120$ dB/Hz$^{2/3}$ have been achieved [7]. While these are very impressive results for MWP-link only used for signal transport and distribution, it is critical to combine link optimization techniques with the advanced functionalities for practical deployment in RF systems. With comb-based filters, link gains of -0.5 dB have been achieved [20]. Recent progress in the optimization of chip-based microwave photonics functionalities are summarized below:

A. Link Gain Optimization Using a Ring Resonator With SBS

The use of RF interference to realize notch filter has the advantage of enabling high extinction ratios within the stopband due to the perfect signal cancellation, however there is partial destructive interference in the passband limiting the link gain to ~ -30 dB [15] due to the existing broadband π-phase difference of the two sidebands. To overcome this, if an optical processor possessing a localized π-phase- offset at one point is used on one sideband of an intensity modulated link, then in principle the condition for destructive interference: equal amplitude and localized π-offset can be met at only one point as shown in Fig. 2 (a), while the constructive interference (between the two sidebands and the carrier) in the passband results in a 6-dB improvement in the link gain, compared to the filter based on a single-sideband configuration. To achieve this localized phase response, the complementary optical responses of the ring resonator and SBS gain are deployed. An over-coupled (OC) ring resonator has a sharp phase response from 0 to 2π passing through π at the resonance center with a non-flat amplitude response as shown in Fig. 2 (b) [21]. This suppression in the amplitude response can be compensated using the response from the SBS gain as shown in Fig. 2 (c), and the slope of the phase response can also be increased. Ideally, the resulting amplitude and phase response is shown in Fig. 2 (d) which is a multiplication product of the transfer functions shown in Fig. 2 (b) and Fig. 2 (c). The amplitude response is now flat, with a sharp phase response going through π at the notch frequency.

Using this technique, a silicon nitride (SiN) OC ring was cascaded with fiber-based SBS to realize filters with a link

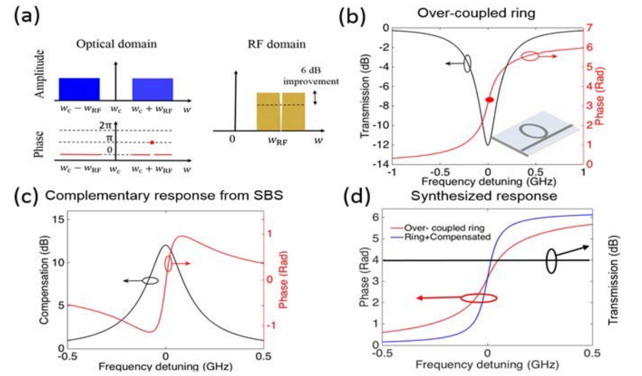

Fig. 2. (a) The concept of RF interference, using intensity modulation achieved by putting a "phase-only" response on one sideband, (b) the amplitude and phase response of the over-coupled ring resonator, (c) the amplitude and the phase response of SBS, and (d) the resultant amplitude and phase response from the multiplication of the transfer functions shown in (b) and (c).

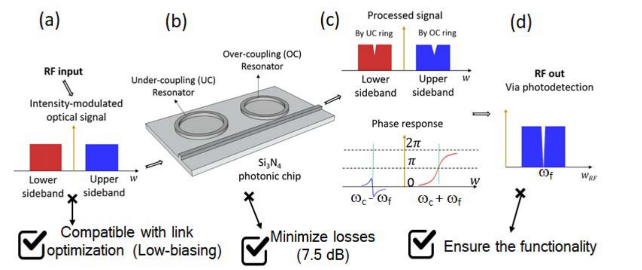

Fig. 3. The principle of operation of the cascaded ring resonator filter (a) an intensity modulated signal is used, (b) the cascaded low-loss Si_3N_4 ring resonators, (c) the processed sidebands and the phase response of the rings, and, (d) a high-suppression RF photonic notch filter.

gain of >0 dB and bandwidth reconfiguration from 100 MHz to 220 MHz achieved by tailoring the SBS gain bandwidth, and a filter tuning range from 1-11 GHz [21]. One can note that the introduced SBS noise only exists in the stopband, which will not lead to additional noise to the filter passband. In this work, the noise figure was not optimized, and an optical amplifier was inserted just before the photodetector, thus increasing the noise figure due to the high spontaneous noise.

B. All-Metric Optimization Using Two SiN Ring Resonators

An improvement in the metrics of on-chip microwave photonic filters was achieved using cascaded SiN ring resonators, with one operated in the over-coupled regime and the other in the under-coupled (UC) regime. This configuration relaxed the power requirements of the filter discussed in IV(A), since the SBS in optical fiber was replaced by a ring that did not require any optical pumping. The concept is illustrated in Fig. 3. An intensity modulated signal (Fig. 3 (a)) is processed by the low-loss photonic chip (Fig. 3 (b)), where the UC ring processes the lower sideband and the OC ring processes the upper sideband (Fig. 3 (c)). At photodetection, the amplitudes of the two optical sidebands are matched on both sidebands at the filter frequency (ω_f), while the OC ring has a phase of π and the UC ring has a phase of 0 at the resonance frequency. Therefore, destructive interference occurs at ω_f resulting in a high-suppression RF photonic notch filter (Fig. 3 (d)).

With this integrated photonic processor, an optimized scheme with two optical amplifiers as shown in Fig. 1 (b)

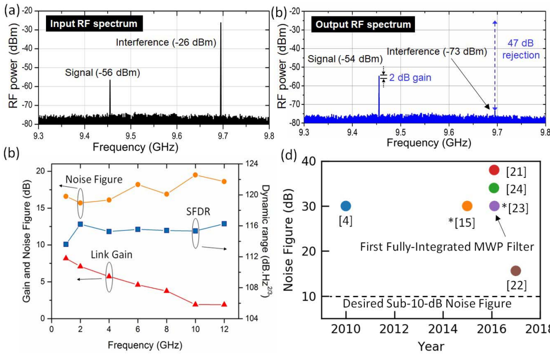

Fig. 4. (a) and (b) Demonstration of the narrowband filtering. A strong interfering signal is rejected while the signal of interest is amplified without any RF amplifiers, (c) the G, NF and $SFDR_3$ of the filter, and (d) a summary of noise figures in various reported IMWP functionalities, * represents estimated values.

was implemented. The output from a laser was amplified to ~1W before being sent through an intensity modulator biased at a low bias angle of $\sim 0.05\,\pi$ enabling low noise operation via the 'low- biasing technique' explained previously. The output from the modulator is then followed by another optical amplifier that compensates for the chip losses and the output signal from the chip is detected by the photodetector. Filter responses with extinction ratios >50 dB were synthesized with bandwidths from 150-300 MHz [22]. To demonstrate the narrowband filtering in a typical crowded spectral environment, a weak RF signal of interest and a strong interferer signal were simultaneously sent to the filter as shown in Fig. 4 (a). When the filter was tuned to the frequency of the interfering signal, a 47 dB rejection can be observed while the signal remarkably experiences 2 dB gain as seen in Fig. 4 (b). The NF, G and the $SFDR_3$ were measured and are shown in Fig. 4 (c). It can be observed that the NF varies between 15.6–19.5 dB, the SFDR varies from 113-116 dB/Hz$^{2/3}$ and positive link gain is observed across the operating bandwidth of the filter.

This result for the first time optimizes the underlying performance metrics of the link while maintaining the full filter functionality. Along with the development of high power on-chip lasers, and efficient integrated modulators and detectors, this technique demonstrates a viable translation pathway of IMWP devices for practical wireless applications [25].

V. Conclusion

There has been considerable progress made in integrated microwave photonics in the last two decades with several key demonstrations, especially in the field of Brillouin-based devices for high-resolution RF signal processing. However, there has been a recent focus on optimizing performance metrics. In this letter, we have presented an overview of optimizing the performance of the functionalities. These include minimizing spontaneous noise in Brillouin-based IMWP devices by using low SBS gain or SBS loss responses, optimizing the underlying analog photonic link through low-biasing techniques and careful amplification distribution strategies along the link. Fig. 4 (d) shows the considerable progress made in IMWP functionality NF metrics in the last decade. The combination of advanced integration technologies [23] with link optimization techniques can enable the realization of all-integrated high-performance microwave photonic devices, which will be an important milestone for the field of integrated microwave photonics.

References

[1] J. Capmany and D. Novak, "Microwave photonics combines two worlds," *Nature Photon.*, vol. 1, no. 6, pp. 319–330, Apr. 2007.

[2] J. Yao, "Microwave photonics," *J. Lightw. Technol.*, vol. 27, no. 3, pp. 314–335, Feb. 1, 2009.

[3] D. Marpaung, C. Roeloffzen, R. Heideman, A. Leinse, S. Sales, and J. Capmany, "Integrated microwave photonics," *Lasers Photon. Rev.*, vol. 7, no. 4, pp. 506–538, Jul. 2013.

[4] K.-Y. Tu *et al.*, "Silicon RF-photonic filter and down-converter," *J. Lightw. Technol.*, vol. 28, no. 20, pp. 3019–3028, Oct. 15, 2010.

[5] M. Merklein *et al.*, "Stimulated Brillouin scattering in photonic integrated circuits: Novel applications and devices," *IEEE J. Sel. Topics Quantum Electron.*, vol. 22, no. 2, pp. 336–346, Mar. 2016.

[6] Y. Souidi, F. Taleb, J. Zheng, M. W. Lee, F. D. Burck, and V. Roncin, "Low-noise and high-gain Brillouin optical amplifier for narrowband active optical filtering based on a pump-to-signal optoelectronic tracking," *Appl. Opt.*, vol. 55, no. 2, pp. 248–253, 2016.

[7] V. J. Urick, J. D. McKinney, and K. J. Williams, *Fundamentals of Microwave Photonics*, vol. 1. Hoboken, NJ, USA: Wiley, 2015.

[8] S. Gundavarapu *et al.* (2017). "Integrated waveguide Brillouin laser." [Online]. Available: https://arxiv.org/abs/1709.04512

[9] R. Van Laer, B. Kuyken, D. Van Thourhout, and R. Baets, "Interaction between light and highly confined hypersound in a silicon photonic nanowire," *Nature Photon.*, vol. 9, no. 3, pp. 199–203, Mar. 2015.

[10] R. Pant *et al.*, "On-chip stimulated Brillouin scattering," *Opt. Express*, vol. 19, no. 9, pp. 8285–8290, Apr. 2011.

[11] A. Choudhary *et al.*, "Advanced integrated microwave signal processing with giant on-chip Brillouin gain," *J. Lightw. Technol.*, vol. 35, no. 4, pp. 846–854, Feb. 15, 2017.

[12] I. Aryanfar *et al.*, "Signal interference RF photonic bandstop filter," *Opt. Express*, vol. 24, no. 13, pp. 14995–15004, 2016.

[13] A. Choudhary *et al.*, "Tailoring of the Brillouin gain for on-chip widely tunable and reconfigurable broadband microwave photonic filters," *Opt. Lett.*, vol. 41, no. 3, pp. 436–439, Feb. 2016.

[14] A. Choudhary *et al.*, "High-resolution, on-chip RF photonic signal processor using Brillouin gain shaping and RF interference," *Sci. Rep.*, vol. 7, p. 5932, Jul. 2017.

[15] D. Marpaung *et al.*, "Low-power, chip-based stimulated Brillouin scattering microwave photonic filter with ultrahigh selectivity," *Optica*, vol. 2, no. 2, pp. 76–83, Feb. 2015.

[16] I. Aryanfar *et al.*, "Reconfigurable microwave bandstop filter based on stimulated Brillouin scattering in a photonic chip," in *Proc. CLEO*, San Jose, CA, USA, 2016, Paper SF1G.7.

[17] C. Feng, S. Preussler, and T. Schneider, "Sharp tunable and additional noise-free optical filter based on Brillouin losses," *Photon. Res.*, vol. 6, no. 2, pp. 132–137, 2018.

[18] A. Choudhary, Y. Liu, D. Marpaung, and B. J. Eggleton, "Brillouin filtering with enhanced noise performance and linearity using anti-Stokes interactions," in *Proc. CLEO*, 2018, Paper STu4F.2.

[19] E. A. Kittlaus, P. Kharel, N. T. Otterstrom, Z. Wang, and P. T. Rakich, "RF-photonic filters via on-chip photonic–phononic emit–receive operations," *J. Lightw. Technol.*, vol. 36, no. 13, pp. 2803–2809, Jul. 1, 2018.

[20] H. J. Kim, A. Rashidinejad, and A. M. Weiner, "Low-loss ultrawideband programmable RF photonic phase filter for spread spectrum pulse compression," *IEEE Trans. Microw. Theory Techn.*, vol. 63, no. 12, pp. 4178–4187, Dec. 2015.

[21] Y. Liu, D. Marpaung, A. Choudhary, and B. J. Eggleton, "Lossless and high-resolution RF photonic notch filter," *Opt. Lett.*, vol. 41, no. 22, pp. 5306–5309, Nov. 2016.

[22] Y. Liu, J. Hotten, A. Choudhary, B. J. Eggleton, and D. Marpaung, "All-optimized integrated RF photonic notch filter," *Opt. Lett.*, vol. 42, no. 22, pp. 4631–4634, 2017.

[23] J. S. Fandiño, P. Muñoz, D. Doménech, and J. Capmany, "A monolithic integrated photonic microwave filter," *Nature Photon.*, vol. 11, pp. 124–129, Dec. 2016.

[24] A. Savchenkov, V. Ilchenko, E. Dale, D. Seidel, A. Matsko, and L. Maleki, "Agile high-*Q* RF photonic zooming filter," *IEEE Photon. Technol. Lett.*, vol. 28, no. 1, pp. 43–46, Jan. 1, 2016.

[25] K. J. Williams, "Signal processing subsystems for RF photonics," in *Proc. OFC*, 2017, Paper W4B.1.